2017 International Conference on
Unmanned Aircraft Systems (ICUAS)
June 13-16, 2017, Miami, FL, USA

A New Framework for UAV-based Remote Sensing Data Processing and Its Application in Almond Water Stress Quantification

Tiebiao Zhao
Mechatronics, Embedded Systems and Automation Lab
University of California, Merced
Merced, California 95343
Email: tzhao3@ucmerced.edu

David Doll
University of California,Cooperative Extension
Merced, California, 95341-6445
Email: dadoll@ucanr.edu

Dong Wang
USDA-ARS Water Management Research Unit
San Joaquin Valley Agricultural Sciences Center
Parlier, California 93648
Email: dong.wang@ars.usda.gov

YangQuan Chen
Mechatronics, Embedded Systems and Automation Lab
University of California, Merced
Merced, California, 95341-6445
Email: ychen53@ucmerced.edu

***Abstract*—With the rapid development of small imaging sensors and unmanned aerial vehicles (UAVs), remote sensing is undergoing a revolution with greatly increased spatial and and temporal resolutions. While more relevant detail becomes available, it is a challenge to analyze the large number of images to extract useful information. This research introduces a new general framework to process high-resolution multi-spectral images based on Principle Component Analysis (PCA) for crop stress quantification. As a case study, this framework is applied in almond water stress quantification using UAV-based remote sensing images. First, crop distributions of pixel value of sample trees are obtained as histograms consisted of 255 bins, assuming the stress information lies in the overall canopy pixels and ignoring the spatial relations among pixels. Second, PCA is applied to extract principle components out of histograms of 255 dimensions. This approach is advantageous in that it makes no assumption about the underlying canopy distribution of pixel values. It is shown that the first principle component has a significant correlation with stem water potential. This method is also compared with the traditional method of using the mean values of canopy Normalized Difference Vegetation Index (NDVI) as a baseline, and it shows improved performance in predicting the water stress.**

I. Introduction

The plummeting cost of imaging sensors and UAVs has ushered high-resolution imaging into a new era. Resolution can have three meanings: spatial resolution, spectral resolution and temporal resolution [1]. High-resolution imaging has been applied in different spatial scale and time scale, from cell levels to plant levels and from seconds to days[2], to monitor plant phenotype and identify the effects of either genotype differences or environmental conditions [3].

However, to meet with these opportunities, there is a big challenge to analyze this high-dimension data [3], [4], [5]. According to the curse-of-dimensionality, the number of training samples will increase exponentially with the increasing number of dimensions [6]. For field experiments, this means the effort to collect ground-truth measurements will be increased exponentially, which is impossible under the limited research resources and not practical in agricultural industries. Therefore it is a must to develop image processing algorithms to extract relevant information from high-dimension data to the considered application.

So far, the most popular way is to average all these pixel values within the region of interest. For example [7], thermal images with a resolution of 1.6 cm/pixel was used to detect water stress in a vineyard and a cotton field. Crop Water Stress Index (CWSI) obtained from average temperature was correlated significantly with both SWP and stomatal conductance. It was shown that regression coefficients based on coldest 33% histogram fraction were similar as those using 100% pixels in vine grapes, showing no extra benefits with image segmentation of sunlit or shaded parts. In [8], a relationship was shown between the mean temperature and the mean spectral reflectance in the Photochemical Reflectance Index (PRI) region between 520 and 580 nm for each variety plot. In [9], Normalized Photochemical Reflectance Index (PRI_{Norm}) yielded a relationship of $R^2 = 0.77, p < 0.01$ against CWSI based on mean pure-vine temperature. In [10], mean crown Chlorophyll fluorescence showed a good relationship with stomatal conductance ($R^2 = 0.67, p < 0.05$) and water potential ($R^2 = 0.66, p < 0.01$). It also showed no significance between NDVI and water potential, which agrees with results in [11], [12].

In addition, higher order statistic moments are also applied to extract information from high-dimension data. There was a good correlation between intra-crown temperature standard

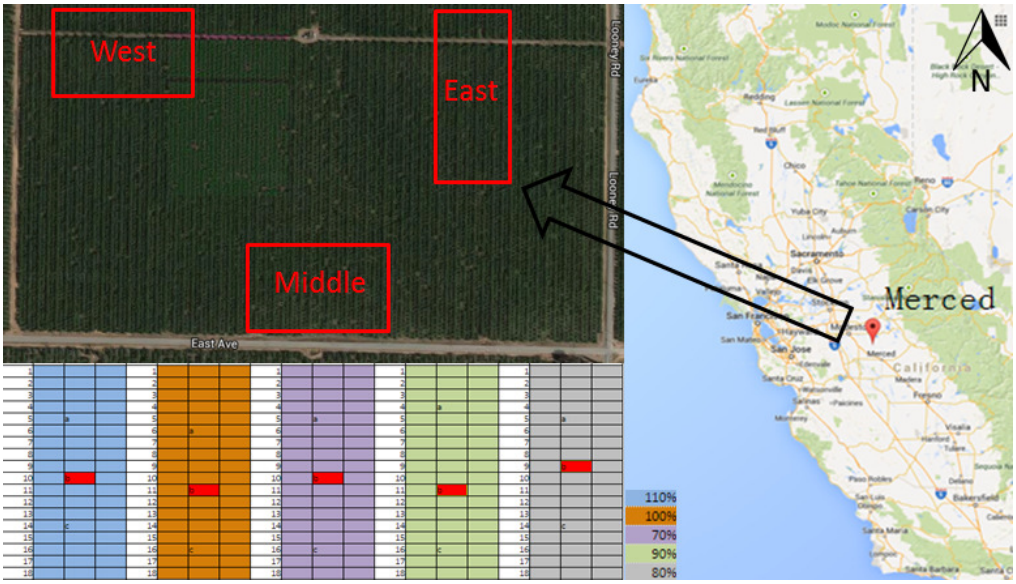

Fig. 1. OVERVIEW OF TESTFIELD, INCLUDING THREE TEST BLOCKS IN THE ORCHARD, EACH COMPOSED OF FIVE PLOTS TREATED WITH 70%, 80%,90%,100%,110% of CROP EVAPTRANSPIRATION.

deviation and water potential while trees had similar canopy temperatures [13]. In NIR region, skewness of canopy distribution showed a good correlation with SWP [14] in almond trees. Similar results applied to Thermal Infrared (TIR) regions, where stressed trees showed a positive skewness of canopy temperature distribution [15], [16].

Therefore, not only absolute pixel values (mean) but also variability tells the crop status information. Imaging based methods provide the possibility to resolve heterogeneity at the levels of canopies, plants or leaves [17], [18], [19], [20], as indicated by measurement distribution. In fact, it has been quite a while to use canopy distribution of temperature [21] or normalized vegetation indices [22] to compare stress levels. Therefore, better stress quantification requires more accurate summarization of canopy distribution. Driven by this question, we propose a PCA based method to extract the dimension capturing the largest variability to reduce the dimension. The methods is further tested using field SWP measurements and flight images and compared with traditional method canopy NDVI mean.

II. Materials Methods

A. Study Areas

The study was carried out in a commercial almond orchard located in Merced County, CA, USA(37.493498°N, -120.634914°W). Three varieties Nonpareil, Carmel, and Monterey were planted on Lovell peach rootstocks 16 years ago at a spacing of 5.5 m×6.1m. The soil of the site is of Rocklin and Greenfield sandy loam. The climate is Mediterranean, characterized by wet, cool, rainy winters and hot,dry summers. The average annual extreme temperature is between 25°F and 30°F. Three blocks were chosen for the study. Each block comprised five different plots, where five irrigation levels are run, one per plot from 70% to 110% of crop evaptranspiration (ET_c) with increment by 10%. Each plot includes three rows of trees with 18 trees per row, as shown in Fig. 1. The water is delivered accordingly by tuning microsprinklers(Supernet, Netafim).

Crop evapotranspiration was calculated according to Food and Agriculture Organization (FAO) method [23].

$$ET_c = K_c * ET_o \tag{1}$$

where ETo is the evapotranspiration rate of a reference surface under optimum treatment and certain climatic conditions, and crop coefficient K_c is defined as the ratio ETc/ETo. K_c utilized in this study was developed in California [24].

B. Field Measurements

Concomitant to each flight and multispectral image acquisition, stem water potential ψ_s were measured with the aim of comparing image-based results with a ground-truthed indicator. The ψ_s of fifteen trees were measured within a block, three trees per irrigation level in the center of the plot, as marked in Fig. 1. One block was measured each week and three blocks were measured in turns. A lower shaded bagged leave was taken from each sample tree and was measured with a pressure chamber (PMS Instrument Model 600, Oregon, USA) following the recommendations [25]. Mention of trade names or commercial products in this publication is solely for the purpose of providing specific information and does not imply recommendation or endorsement by the University of California or U.S. Department of Agriculture.

C. Airborne Imagery

The airborne campaigns were conducted at 60 meters above the ground and the spatial resolution was 1.87 cm/pix. The cameras were triggered at a distance of 16 m to obtain the

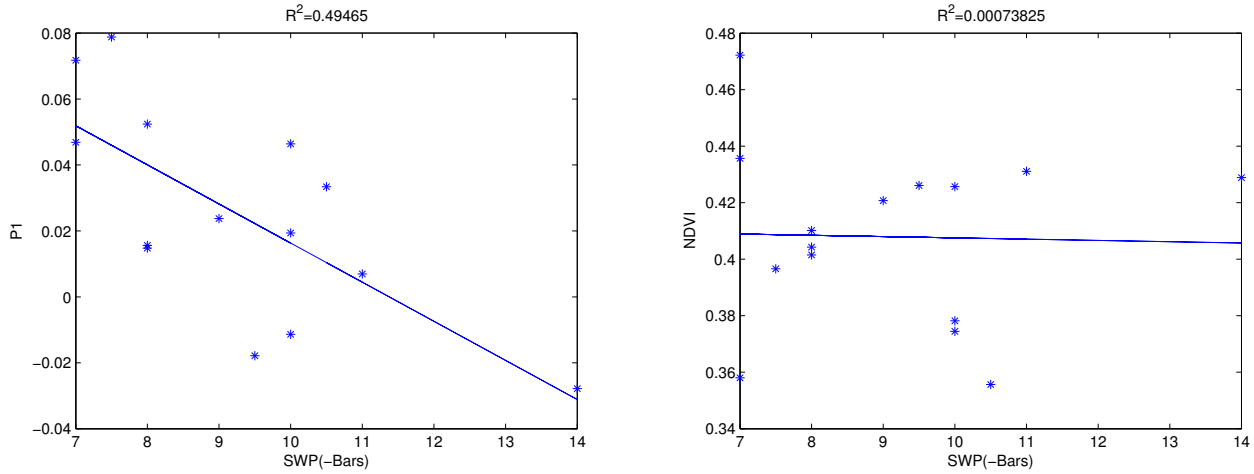

(a) Relationship of the Proposed Method and SWP, 6-12-2015

(b) Relationship of NDVI and SWP, 6-12-2015

Fig. 2. Comparing the Relationship of the Proposed Method and NDVI with SWP Using Data of June, 12, 2015

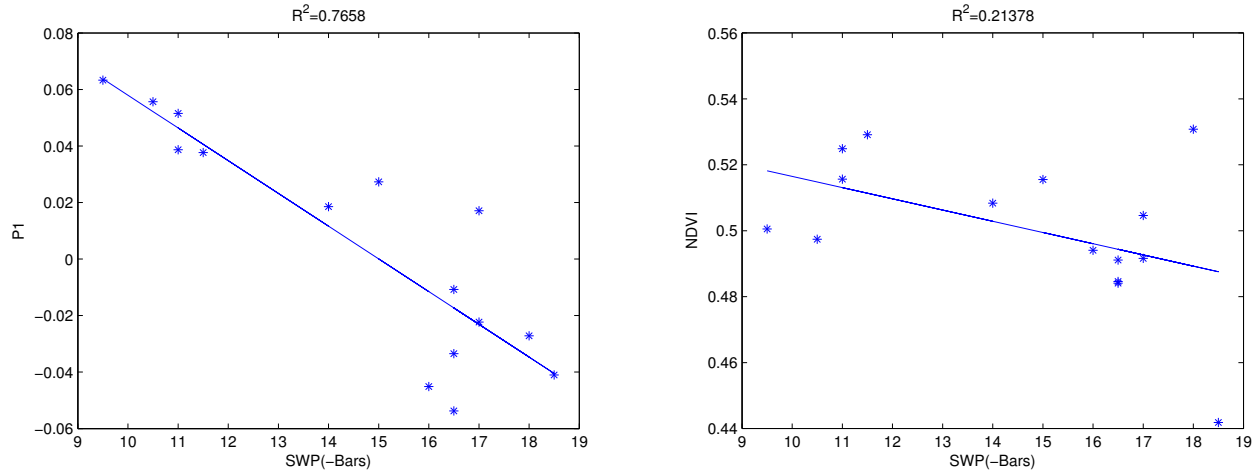

(a) Relationship of the Proposed Method and SWP, 6-18-2015

(b) Relationship of NDVI and SWP, 6-18-2015

Fig. 3. Comparing the Relationship of the Proposed Method and NDVI with SWP Using Data of June, 18, 2015

overlap up to 75% in order to stitch images using the software PhotoScan (Agisoft,Russia). The images of white panels and dark panels were taken right before flight missions serving as reflectance references. The digital number(DN) value of raw image is converted to reflectance with an empirical method [26] as shown in Eqn.2. The DN of dark panels (DN_D) and white panels (DN_W) are determined by the point located in the central part of its histogram. NDVI is calculated according to Eqn.3, where the reflectance in the red band (ρ_R) is replaced with that of the blue band (ρ_B). It is reasonable because the distance between objects and cameras is 60 meters and atmosphere scattering and absorption would not have a significant effect in the blue band. Most importantly, this saves effort to register the images between bands and decreases error from low regeneration accuracy.

To minimize the influence of bidirectional reflectance distribution function (BRDF) effects [27], only the canopy images collected with nadir view angles were used. Then the canopy image of each sample tree was separated from soil manually and the pixels within the canopy were further analyzed.

$$\rho_\lambda = \frac{DN - DN_D}{DN_W - DN_D} \tag{2}$$

$$NDVI = \frac{\rho_{NIR} - \rho_B}{\rho_{NIR} + \rho_B}. \tag{3}$$

D. Proposed Framework

First, canopy distribution of pixel difference between NIR band and blue band is calculated. Histograms of 15 sample tree canopies are obtained. Because the sizes of these sample trees are different, the numbers of canopy pixels for each sample tree are different. Second, the histograms are

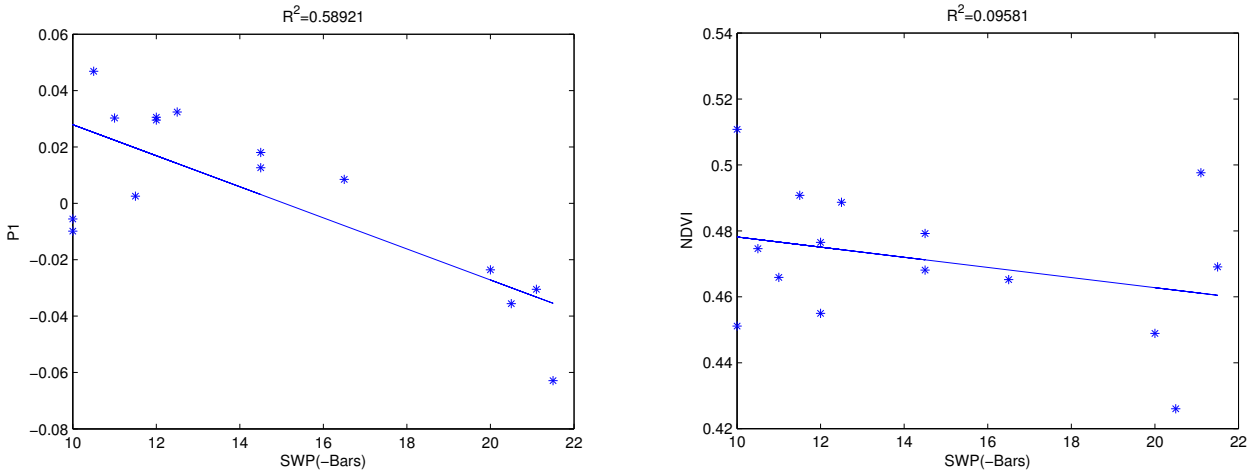

(a) Relationship of the Proposed Method and SWP, 8-20-2015

(b) Relationship of NDVI and SWP, 8-20-2015

Fig. 4. Comparing the Relationship of the Proposed Method and NDVI with SWP Using Data of August, 20, 2015

normalized with the total number of pixels within canopies. Third, PCA is applied to extract the principle component, which explains the largest variance of normalized canopy distributions of 15 sample trees. Finally, the first principle component is used for correlation analysis with SWP. Better descriptions step by step are as follows.

1) For the sample tree $m = 1, 2, ..., 15$, obtain the difference image between NIR and blue bands, denoted as I_m composed of the element

$$i_{m,jk} = nir_{m,jk} - b_{m,jk} \tag{4}$$

where $nir_{m,jk}$, $b_{m,jk}$ are the pixel value ranging between 0 and 255 in the jth row and kth column in NIR band, blue band respectively.

2) Obtain its histograms

$$H_m = [h_{m,1}, h_{m,2}, ..., h_{m,244}, h_{m,245}] \tag{5}$$

where $h_{m,i}, i = 1, 2, ..., 255$ is the number of pixels with the value i.

3) Calculate the number of pixels within the canopy, denoted as

$$S_m = h_{m,1} + h_{m,2} + ... + h_{m,244} + h_{m,245} \tag{6}$$

4) Normalize the histograms using S_m, obtain

$$NH_m = H_m/S_m = [nh_{m,1}, nh_{m,2}, ..., nh_{m,255}] \tag{7}$$

5) Reorganize the histograms of these 15 sample trees, obtain

$$X = \begin{bmatrix} nh_{1,1} & nh_{1,2} & ... & nh_{1,255} \\ nh_{2,1} & nh_{2,2} & ... & nh_{2,255} \\ ... & & & \\ nh_{15,1} & nh_{15,2} & ... & nh_{15,255} \end{bmatrix}$$

6) Apply PCA to matrix X, obtain the first principle component for each sampe tree and conduct the correlation analysis between P and Ψ

$$P = \begin{bmatrix} p_{1,1} \\ p_{2,1} \\ ... \\ p_{14,1} \\ p_{15,1} \end{bmatrix}, \Psi = \begin{bmatrix} \psi_1 \\ \psi_2 \\ ... \\ \psi_{14} \\ \psi_{15} \end{bmatrix}$$

where $p_{m,1}$ is the first principle component and ψ_m is SWP measurement for the sample tree m.

III. Results and Discussions

A. Performance Comparison With NDVI Mean

As a base line, canopy NDVI mean is compared with the proposed methods. Data collected within three weeks are used for analysis. The results are shown in Fig. 2, Fig. 3 and Fig. 4, indicating the proposed methods performs better than traditional canopy NDVI mean. Table. I shows the statistics of modeling parameters. It demonstrates that the correlations between first principle component and SWP are significant ($p < 0.01$).

B. Relationship With Non-normalized NDVI Mean

In [12], Non-normalized NDVI (NNDVI) was proposed to quantify water stress and correlated well with SWP measurements. In fact, under the the proposed framework, NNDVI is a special case if we design the coefficient in the following way.

$$M_{coef} = \begin{bmatrix} 1 \\ 2 \\ ... \\ 254 \\ 255 \end{bmatrix}_{255\times 1}$$

By multiplying X with M_{coef}, NNDVI vegetation index is obtained. Here the proposed method extracts the dimension

TABLE I
MODELING PERFORMANCE PARAMETERS USING PROPOSED METHODS WITHIN THREE DIFFERENT DAYS

Parameters	06-12-2015	06-18-2015	08-20-2015
R^2	0.49465	0.7658	0.58921
pValue (Intercept)	6.8796e-11	1.2717e-14	3.6002e-11
pValue (P1)	0.0050114	1.9426e-05	0.00083472

maintaining the largest variance using coefficient matrix obtained by PCA.

IV. Conclusion and Future Work

Assuming that spatial relationship among pixels do not tell stress information about the plant canopy, we quantify the plant water stress based on more accurate description of canopy distribution, while minimizing the dimensions of extracted features. A general framework of dimension reduction is proposed to extract relevant information from high-dimension canopy distribution. As the most popular dimension reduction technique, PCA is applied to test this framework with the measurements collected within three different weeks. Better performance is obtained to explain the trend of SWP using the proposed method. Intrinsically, PCA is a linear dimension reduction technique, so it is promising to apply nonlinear techniques to obtain better results, especially considering the complexity of plant systems for future work.

Acknowledgment

Thanks go to Andrew Ray for field measurements collections and Larry Burrow for lending his expertise in almond orchard. Thanks go to MESA Lab Scientific Data Drone crew members Ph.D. students Brandon Stark and Brendan Smith, undergraduate researchers Yoni Shchemelinin, Andreas Anderson and Jacob Clark for contributions in conducting flight missions in the 2015 growing season.

References

[1] J. A. Benediktsson, J. Chanussot, and W. M. Moon, "Very high-resolution remote sensing: Challenges and opportunities [point of view]," *Proceedings of the IEEE*, vol. 100, no. 6, pp. 1907–1910, 2012.

[2] S. Dhondt, N. Wuyts, and D. Inzé, "Cell to whole-plant phenotyping: the best is yet to come," *Trends in plant science*, vol. 18, no. 8, pp. 428–439, 2013.

[3] M. Minervini, H. Scharr, and S. A. Tsaftaris, "Image analysis: the new bottleneck in plant phenotyping [applications corner]," *IEEE Signal Processing Magazine*, vol. 32, no. 4, pp. 126–131, 2015.

[4] L. Li, Q. Zhang, and D. Huang, "A review of imaging techniques for plant phenotyping," *Sensors*, vol. 14, no. 11, pp. 20 078–20 111, 2014.

[5] E. P. Spalding and N. D. Miller, "Image analysis is driving a renaissance in growth measurement," *Current Opinion in Plant Biology*, vol. 16, no. 1, pp. 100–104, 2013.

[6] R. E. Bellman, *Adaptive control processes: a guided tour*. Princeton university press, 2015.

[7] M. Meron, M. Sprintsin, J. Tsipris, V. Alchanatis, and Y. Cohen, "Foliage temperature extraction from thermal imagery for crop water stress determination," *Precision Agriculture*, vol. 14, no. 5, pp. 467–477, 2013.

[8] J. A. Berni, P. J. Zarco-Tejada, L. Suárez, and E. Fereres, "Thermal and narrowband multispectral remote sensing for vegetation monitoring from an unmanned aerial vehicle," *Geoscience and Remote Sensing, IEEE Transactions on*, vol. 47, no. 3, pp. 722–738, 2009.

[9] P. J. Zarco-Tejada, V. González-Dugo, L. Williams, L. Suárez, J. A. Berni, D. Goldhamer, and E. Fereres, "A pri-based water stress index combining structural and chlorophyll effects: Assessment using diurnal narrow-band airborne imagery and the cwsi thermal index," *Remote sensing of environment*, vol. 138, pp. 38–50, 2013.

[10] P. J. Zarco-Tejada, V. González-Dugo, and J. A. J. Berni, "Fluorescence, temperature and narrow-band indices acquired from a UAV platform for water stress detection using a micro-hyperspectral imager and a thermal camera," *Remote Sensing of Environment*, vol. 117, pp. 322–337, 2012.

[11] T. Zhao, B. Stark, Y. Chen, A. L. Ray, and D. Doll, "A detailed field study of direct correlations between ground truth crop water stress and normalized difference vegetation index (ndvi) from small unmanned aerial system (suas)," in *Unmanned Aircraft Systems (ICUAS), 2015 International Conference on*. IEEE, 2015, pp. 520–525.

[12] T. Zhao, B. Stark, Y. Chen, A. Ray, and D. Doll, "More reliable crop water stress quantification using small unmanned aerial systems (suas)," *IFAC-PapersOnLine*, vol. 49, no. 16, pp. 409–414, 2016.

[13] V. Gonzalez-Dugo, P. Zarco-Tejada, J. A. Berni, L. Suárez, D. Goldhamer, and E. Fereres, "Almond tree canopy temperature reveals intra-crown variability that is water stress-dependent," *Agricultural and Forest Meteorology*, vol. 154, pp. 156–165, 2012.

[14] T. Zhao, D. David, D. Wang, and Y. Chen, "Quantifying almond water stress using unmanned aerial vehicles (uavs): correlation of stem water potential and higher order moments of non-normalized canopy distribution," in *ASME 2017 International Design Engineering Technical Conferences & Computers and Information in Engineering Conference*. ASME, 2017, Submitted.

[15] A. Matese, P. Toscano, S. F. Di Gennaro, L. Genesio, F. P. Vaccari, J. Primicerio, C. Belli, A. Zaldei, R. Bianconi, and B. Gioli, "Intercomparison of uav, aircraft and satellite remote sensing platforms for precision viticulture," *Remote Sensing*, vol. 7, no. 3, pp. 2971–2990, 2015.

[16] H. Zheng, X. Zhou, T. Cheng, X. Yao, Y. Tian, W. Cao, and Y. Zhu, "Evaluation of a uav-based hyperspectral frame camera for monitoring the leaf nitrogen concentration in rice," in *Geoscience and Remote Sensing Symposium (IGARSS), 2016 IEEE International*. IEEE, 2016, pp. 7350–7353.

[17] L. Chaerle and D. Van Der Straeten, "Seeing is believing: imaging techniques to monitor plant health," *Biochimica et Biophysica Acta (BBA)-Gene Structure and Expression*, vol. 1519, no. 3, pp. 153–166, 2001.

[18] S. Lenk, L. Chaerle, E. E. Pfündel, G. Langsdorf, D. Hagenbeek, H. K. Lichtenthaler, D. Van Der Straeten, and C. Buschmann, "Multispectral fluorescence and reflectance imaging at the leaf level and its possible applications," *Journal of Experimental Botany*, vol. 58, no. 4, pp. 807–814, 2007.

[19] L. Chaerle, S. Lenk, I. Leinonen, H. G. Jones, D. Van Der Straeten, and C. Buschmann, "Multi-sensor plant imaging: Towards the development of a stress-catalogue," *Biotechnology Journal*, vol. 4, no. 8, pp. 1152–1167, 2009.

[20] B. Berger, B. Parent, and M. Tester, "High-throughput shoot imaging to study drought responses," *Journal of experimental botany*, p. erq201, 2010.

[21] M. Fuchs, "Infrared measurement of canopy temperature and detection of plant water stress," *Theoretical and Applied Climatology*, vol. 42, no. 4, pp. 253–261, 1990.

[22] S. Candiago, F. Remondino, M. De Giglio, M. Dubbini, and M. Gattelli, "Evaluating multispectral images and vegetation indices for precision farming applications from uav images," *Remote Sensing*, vol. 7, no. 4, pp. 4026–4047, 2015.

[23] R. G. Allen, L. S. Pereira, D. Raes, M. Smith *et al.*, "Crop evapotranspiration-guidelines for computing crop water requirements-fao irrigation and drainage paper 56," *FAO, Rome*, vol. 300, no. 9, p. D05109, 1998.

[24] D. Doll and K. Shackel, "Drought management for california almonds," *Crops and Soils*, vol. 49, no. 2, pp. 28–35, 2016.

[25] A. Fulton, J. Grant, R. Buchner, and J. Connell, "Using the pressure chamber for irrigation management in walnut, almond, and prune," *Oakland: University of California Division of Agriculture and Natural Resources Publication*, vol. 8503, 2014.

[26] G. M. Smith and E. J. Milton, "The use of the empirical line method

to calibrate remotely sensed data to reflectance," *International Journal of remote sensing*, vol. 20, no. 13, pp. 2653–2662, 1999.

[27] B. Stark, T. Zhao, and Y. Chen, "An analysis of the effect of the bidirectional reflectance distribution function on remote sensing imagery accuracy from small unmanned aircraft systems," in *Unmanned Aircraft Systems (ICUAS), 2016 International Conference on*. IEEE, 2016, pp. 1342–1350.